PHYSICAL REVIEW D, VOLUME 63, 031103(R)

Study of $B \to \psi(2S)K$ and $B \to \psi(2S)K^*(892)$ decays

S. J. Richichi, H. Severini, P. Skubic, and A. Undrus
University of Oklahoma, Norman, Oklahoma 73019

S. Chen, J. Fast, J. W. Hinson, J. Lee, D. H. Miller, E. I. Shibata, I. P. J. Shipsey, and V. Pavlunin
Purdue University, West Lafayette, Indiana 47907

D. Cronin-Hennessy, A. L. Lyon, and E. H. Thorndike
University of Rochester, Rochester, New York 14627

C. P. Jessop, H. Marsiske, M. L. Perl, V. Savinov, and X. Zhou
Stanford Linear Accelerator Center, Stanford University, Stanford, California 94309

T. E. Coan, V. Fadeyev, Y. Maravin, I. Narsky, R. Stroynowski, J. Ye, and T. Wlodek
Southern Methodist University, Dallas, Texas 75275

M. Artuso, R. Ayad, C. Boulahouache, K. Bukin, E. Dambasuren, S. Karamov, G. Majumder, G. C. Moneti, R. Mountain, S. Schuh, T. Skwarnicki, S. Stone, G. Viehhauser, J. C. Wang, A. Wolf, and J. Wu
Syracuse University, Syracuse, New York 13244

S. Kopp
University of Texas, Austin, Texas 78712

A. H. Mahmood
University of Texas-Pan American, Edinburg, Texas 78539

S. E. Csorna, I. Danko, K. W. McLean, Sz. Márka, and Z. Xu
Vanderbilt University, Nashville, Tennessee 37235

R. Godang, K. Kinoshita,* I. C. Lai, and S. Schrenk
Virginia Polytechnic Institute and State University, Blacksburg, Virginia 24061

G. Bonvicini, D. Cinabro, S. McGee, L. P. Perera, and G. J. Zhou
Wayne State University, Detroit, Michigan 48202

E. Lipeles, S. P. Pappas, M. Schmidtler, A. Shapiro, W. M. Sun, A. J. Weinstein, and F. Würthwein†
California Institute of Technology, Pasadena, California 91125

D. E. Jaffe, G. Masek, H. P. Paar, E. M. Potter, S. Prell, and V. Sharma
University of California, San Diego, La Jolla, California 92093

D. M. Asner, A. Eppich, T. S. Hill, R. J. Morrison, and H. N. Nelson
University of California, Santa Barbara, California 93106

R. A. Briere and G. P. Chen
Carnegie Mellon University, Pittsburgh, Pennsylvania 15213

B. H. Behrens, W. T. Ford, A. Gritsan, J. Roy, and J. G. Smith
University of Colorado, Boulder, Colorado 80309-0390

J. P. Alexander, R. Baker, C. Bebek, B. E. Berger, K. Berkelman, F. Blanc, V. Boisvert, D. G. Cassel, M. Dickson, P. S. Drell, K. M. Ecklund, R. Ehrlich, A. D. Foland, P. Gaidarev, L. Gibbons, B. Gittelman, S. W. Gray, D. L. Hartill, B. K. Heltsley, P. I. Hopman, C. D. Jones, J. Kandaswamy, D. L. Kreinick, M. Lohner, A. Magerkurth, T. O. Meyer, N. B. Mistry, E. Nordberg, J. R. Patterson, D. Peterson, D. Riley, J. G. Thayer, D. Urner, B. Valant-Spaight, and A. Warburton
Cornell University, Ithaca, New York 14853

P. Avery, C. Prescott, A. I. Rubiera, J. Yelton, and J. Zheng
University of Florida, Gainesville, Florida 32611

G. Brandenburg, A. Ershov, Y. S. Gao, D. Y.-J. Kim, and R. Wilson
Harvard University, Cambridge, Massachusetts 02138

T. E. Browder, Y. Li, J. L. Rodriguez, and H. Yamamoto
University of Hawaii at Manoa, Honolulu, Hawaii 96822

T. Bergfeld, B. I. Eisenstein, J. Ernst, G. E. Gladding, G. D. Gollin, R. M. Hans, E. Johnson, I. Karliner, M. A. Marsh, M. Palmer, C. Plager, C. Sedlack, M. Selen, J. J. Thaler, and J. Williams
University of Illinois, Urbana-Champaign, Illinois 61801

K. W. Edwards
Carleton University, Ottawa, Ontario, Canada K1S 5B6
and the Institute of Particle Physics, Canada

R. Janicek and P. M. Patel
McGill University, Montréal, Québec, Canada H3A 2T8
and the Institute of Particle Physics, Canada

A. J. Sadoff
Ithaca College, Ithaca, New York 14850

R. Ammar, A. Bean, D. Besson, R. Davis, N. Kwak, and X. Zhao
University of Kansas, Lawrence, Kansas 66045

S. Anderson, V. V. Frolov, Y. Kubota, S. J. Lee, R. Mahapatra, J. J. O'Neill, R. Poling, T. Riehle, A. Smith, C. J. Stepaniak, and J. Urheim
University of Minnesota, Minneapolis, Minnesota 55455

S. Ahmed, M. S. Alam, S. B. Athar, L. Jian, L. Ling, M. Saleem, S. Timm, and F. Wappler
State University of New York at Albany, Albany, New York 12222

A. Anastassov, J. E. Duboscq, E. Eckhart, K. K. Gan, C. Gwon, T. Hart, K. Honscheid, D. Hufnagel, H. Kagan, R. Kass, T. K. Pedlar, H. Schwarthoff, J. B. Thayer, E. von Toerne, and M. M. Zoeller
Ohio State University, Columbus, Ohio 43210

(CLEO Collaboration)

(Received 16 September 2000; published 10 January 2001)

Color-suppressed decays of B mesons to final states with $\psi(2S)$ mesons have been observed with the CLEO detector. The branching fractions for the decays $B^+\to\psi(2S)K^+$, $B^+\to\psi(2S)K^*(892)^+$, $B^0\to\psi(2S)K^0$, and $B^0\to\psi(2S)K^*(892)^0$ are measured to be $(7.8\pm0.7\pm0.9)\times10^{-4}$, $(9.2\pm1.9\pm1.2)\times10^{-4}$, $(5.0\pm1.1\pm0.6)\times10^{-4}$, and $(7.6\pm1.1\pm1.0)\times10^{-4}$, respectively, where the first uncertainty is statistical and the second is systematic. The first measurement of the longitudinal polarization fraction is extracted from the angular analysis of the $B\to\psi(2S)K^*(892)$ candidates: $\Gamma_L/\Gamma=0.45\pm0.11\pm0.04$. Our measurements of the decays $B^0\to\psi(2S)K^0$ and $B^+\to\psi(2S)K^*(892)^+$ are first observations.

DOI: 10.1103/PhysRevD.63.031103 PACS number(s): 13.25.Hw

Studies of the decays of B mesons to $\psi(2S)$-meson final states contribute to knowledge of hadronic B-meson decays, which involve both the weak and strong interactions. The ARGUS Collaboration observed the decay $B^+\to\psi(2S)K^+$ [1] with a branching fraction $(18\pm8\pm4)\times10^{-4}$ and obtained upper limits for the branching fractions of the other $B\to\psi(2S)K^{(*)}$ modes [2]. The CLEO Collaboration subsequently measured the branching fraction $\mathcal{B}(B^+\to\psi(2S)K^+)=(6.1\pm2.3\pm0.9)\times10^{-4}$ and determined more stringent upper limits for the other $B\to\psi(2S)K^{(*)}$ branching fractions [3]. Recently, the Collider Detector at Fermilab (CDF) Collaboration measured the branching fractions $\mathcal{B}(B^+\to\psi(2S)K^+)=(5.6\pm0.8\pm1.0)\times10^{-4}$ and $\mathcal{B}(B^0\to\psi(2S)K^{*0})=(9.2\pm2.0\pm1.6)\times10^{-4}$ [4].

Of the decays $B\to\psi(2S)K^{(*)}$ [5] reported here, the modes involving a neutral B^0 meson decaying to a CP

*Permanent address: University of Cincinnati, Cincinnati, OH 45221.

†Permanent address: Massachusetts Institute of Technology, Cambridge, MA 02139.

eigenstate can be used, in a manner similar to that for their J/ψ analogues, to measure the CP-violation angle β of the unitarity quark-mixing triangle. Measurements of the modes $B\to\psi(2S)K^{(*)}$ can also contribute to tests of the factorization hypothesis [6] and to phenomenological techniques employed in several models that predict the ratios of vector to pseudoscalar kaon production and the longitudinal polarization fraction in $B\to J/\psi K^{(*)}$ and $B\to\psi(2S)K^{(*)}$ decays [7–11]. Absolute branching fractions have been calculated by combining these phenomenological approaches with inputs from experiments [8]. Nonfactorizable contributions to the decay amplitudes can provide substantial corrections to these predictions [12]. Both improvements in the accuracy of the experimental measurements and the observation of new modes can help in differentiating between models and understanding the role of any nonfactorizable corrections [9–11].

In this Rapid Communication we report measurements of all four decays $B\to\psi(2S)K^{(*)}$, including the first observation of the decays $B^0\to\psi(2S)K^0$ and $B^+\to\psi(2S)K^{*+}$. We also present the first angular analysis of the decays $B^+\to\psi(2S)K^{*+}$ and $B^0\to\psi(2S)K^{*0}$, which leads to a determination of the longitudinal polarization fraction, Γ_L/Γ. The measurements reported in this Rapid Communication supersede the previous CLEO results [3].

The data used in this analysis were collected from e^+e^- collisions on or near the $\Upsilon(4S)$ resonance at the Cornell Electron Storage Ring (CESR) with two configurations of the CLEO detector, CLEO II and CLEO II.V.

In CLEO II [13], the momenta of charged particles were measured in a tracking system consisting of a 6-layer straw-tube chamber, a 10-layer precision drift chamber, and a 51-layer main drift chamber, all operating inside a 1.5 T solenoidal magnet. The main drift chamber also provided a measurement of the specific ionization (dE/dx) of charged particles. For CLEO II.V, the innermost wire chamber was replaced with a three-layer silicon vertex detector [14], and the argon-ethane gas of the main drift chamber was replaced with a helium-propane mixture. A 7800-crystal CsI calorimeter detected photon candidates and was used for electron identification. Muon candidates were identified with proportional counters placed at various depths in the steel absorber. The total integrated luminosity of the data sample at the $\Upsilon(4S)$ energy is 9.2 fb^{-1}, corresponding to the production of 9.7×10^6 $B\overline{B}$ pairs. A data sample of 4.6 fb^{-1} recorded 60 MeV below the $\Upsilon(4S)$ energy was used for continuum non-$B\overline{B}$ background evaluation. The Monte Carlo simulation of the CLEO detector is GEANT-based [15]. Simulated events for the CLEO II and CLEO II.V configurations are processed in the same manner as data.

Candidates for the decays $B^+\to\psi(2S)K^{(*)+}$ and $B^0\to\psi(2S)K^{(*)0}$ are reconstructed via the decays $\psi(2S)\to l^+l^-$ and $\psi(2S)\to J/\psi\pi^+\pi^-\to l^+l^-\pi^+\pi^-$, where l^+l^- stands for e^+e^- or $\mu^+\mu^-$ pairs. The K^{*+} and K^{*0} mesons are reconstructed in their $K^0_S\pi^+$, $K^+\pi^0$, $K^+\pi^-$, and $K^0_S\pi^0$ modes.

Electron candidates are identified by their calorimeter energy deposition, which must be consistent with their measured momenta and specific ionization in the drift chamber. Electrons may be accompanied by radiative photons emitted in the narrow cone along the momentum direction of the electron. The recovery of these photons improves the invariant mass resolution and results in a 20% relative increase in the $\psi(2S)\to l^+l^-$ reconstruction efficiency [16]. At least one muon candidate is required to penetrate five nuclear interaction lengths of material, whereas the other candidate must penetrate at least three nuclear interaction lengths. In the decays $\psi(2S)\to J/\psi\pi^+\pi^-$, the $\pi^+\pi^-$ invariant mass is required to be greater than 0.4 GeV/c^2, as motivated by the measured $\pi^+\pi^-$ invariant mass spectrum [17]. For J/ψ and $\psi(2S)$ candidates in the dielectron final state we use an asymmetric mass criterion to take into account the radiative tail: $-100<M_{e^+e^-}-M_{J/\psi}<50$ MeV/c^2 and $-140<M_{e^+e^-}-M_{\psi(2S)}<60$ MeV/c^2. The dimuon candidate mass is required to be within 50 (60) MeV/c^2 of the J/ψ ($\psi(2S)$) mass.

Candidate K^0_S mesons are reconstructed from pairs of oppositely charged tracks with vertices separated from the primary interaction point with at least 3 standard deviations. Candidate K^* mesons are required to have a $K\pi$ invariant mass within 80 MeV/c^2 of the K^* mass [18]. For the charged kaon candidates from K^* decays, the dE/dx and time-of-flight information (at least one source of identifica-

TABLE I. Dimensions of the ΔE vs $M(B)$ signal area (M_0 is the PDG B-meson mass [18]), number of events in the signal area, background estimates, and detection efficiencies (branching fractions not included).

	$B^+\to\psi(2S)K^+$	$B^0\to\psi(2S)K^0_S$	$B^+\to\psi(2S)K^{*+}$		$B^0\to\psi(2S)K^{*0}$	
			$K^{*+}\to K^0_S\pi^+$	$K^{*+}\to K^+\pi^0$	$K^{*0}\to K^+\pi^-$	$K^{*0}\to K^0_S\pi^0$
$\lvert\Delta E\rvert$ [MeV]	20	20	30	40	30	40
$\lvert M(B)-M_0\rvert$ [MeV/c^2]	8	8	8	9	8	9
$N(\psi(2S)\to l^+l^-)$	60	11	5	7	20	1
$N(\psi(2S)\to J/\psi\pi^+\pi^-)$	69	10	9	2	25	2
$B\to\psi(2S)X$ bkg.	0.2 ± 0.1	0.02 ± 0.02	0.6 ± 0.2	0.3 ± 0.2	1.7 ± 0.5	0.2 ± 0.1
Combinatorial bkg.	1.6 ± 0.5	0.3 ± 0.2	0.5 ± 0.3	0.7 ± 0.3	1.8 ± 0.5	0.1 ± 0.1
Total bkg.	1.8 ± 0.5	0.3 ± 0.2	1.1 ± 0.4	1.0 ± 0.4	3.5 ± 0.7	0.3 ± 0.1
$\epsilon(\psi(2S)\to l^+l^-)$ [%]	44	33	18	6	23	5
$\epsilon(\psi(2S)\to J/\psi\pi^+\pi^-)$ [%]	23	17	8	3	11	3

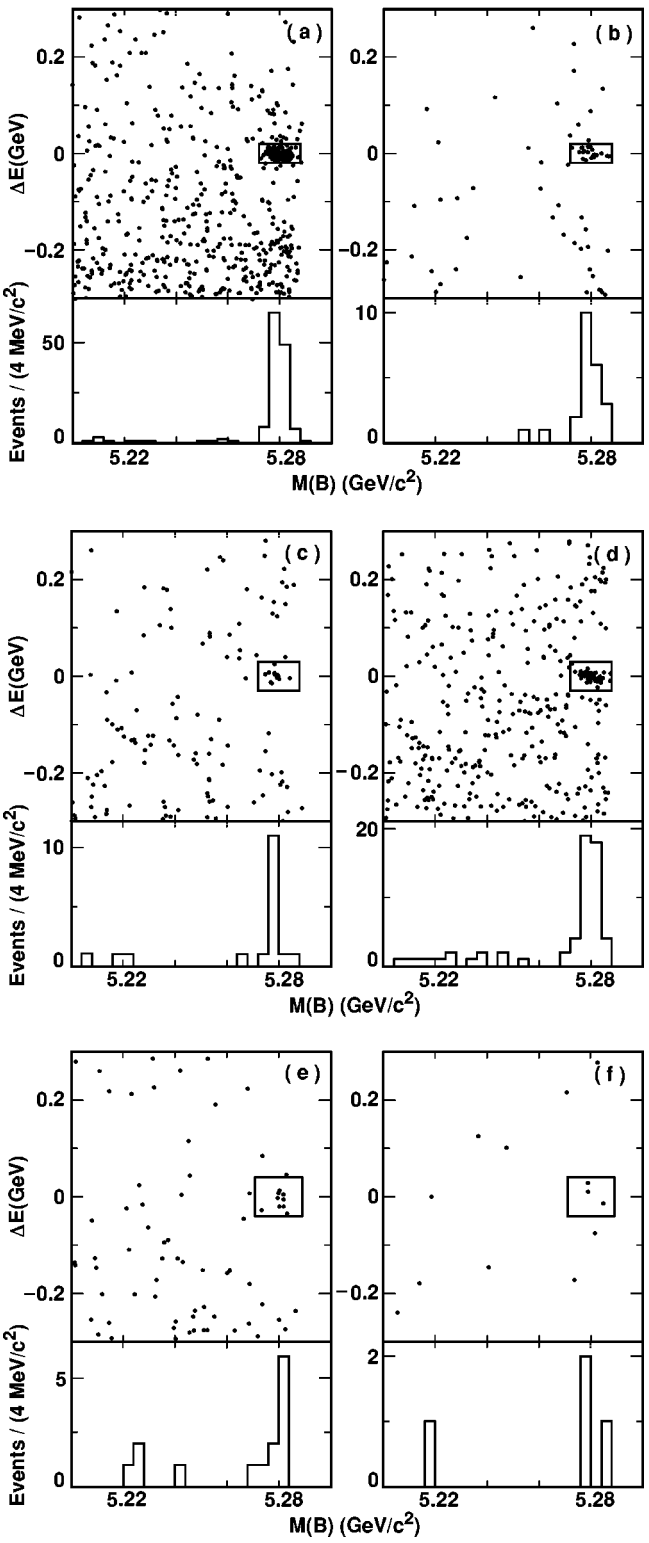

FIG. 1. ΔE vs $M(B)$ for (a) $B^+ \to \psi(2S)K^+$, (b) $B^0 \to \psi(2S)K_S^0$, (c) $B^+ \to \psi(2S)K^{*+}$, $K^{*+} \to K_S^0\pi^+$, (d) $B^0 \to \psi(2S)K^{*0}$, $K^{*0} \to K^+\pi^-$, (e) $B^+ \to \psi(2S)K^{*+}$, $K^{*+} \to K^+\pi^0$, and (f) $B^0 \to \psi(2S)K^{*0}$, $K^{*0} \to K_S^0\pi^0$ candidate events, with the contributions from $\psi(2S) \to l^+l^-$ and $\psi(2S) \to J/\psi\pi^+\pi^-$ combined. The boxes indicate the signal regions. Also shown are the $M(B)$ projections for the candidate events with ΔE within the signal area limits.

tion must be available) must be consistent with a kaon hypothesis to within two standard deviations.

Photon candidates are defined as energy clusters in the calorimeter of at least 60 MeV in the barrel region, $|\cos\theta| < 0.80$, and 100 MeV in the end cap region, $0.80 < |\cos\theta| < 0.95$, where θ is the polar angle with respect to the beam axis. Each photon candidate must have a lateral profile of energy deposition consistent with that expected of a photon. In addition, we do not use the fragments of a nearby large shower as photon candidates. The π^0 candidates are reconstructed from photon pairs with at least one photon from the barrel region and an invariant mass within 3 standard deviations of the PDG π^0 mass [18]. The π^0 mass resolution is calculated from the known angular and energy resolutions of the calorimeter.

For the modes with a neutral pion in the final state, the K^* helicity angle must be greater than $\pi/2$, which effectively eliminates the low momentum neutral pion background. The K^* helicity angle, θ_{K^*}, is the polar angle of the K meson in the K^* rest frame relative to the negative of the $\psi(2S)$ direction in that frame.

The B candidates are selected by means of two parameters: the difference between the energy of the B candidate and the beam energy, $\Delta E \equiv E(\psi(2S)) + E(K^{(*)}) - E_{\rm beam}$, and the beam-constrained B-candidate mass, $M(B) \equiv \sqrt{E_{\rm beam}^2 - \vec{p}_B^{\,2}}$, where $\vec{p}_B$ is the momentum of the B candidate. The B candidate must be within the ± 3 standard deviation signal region (Table I) in the ΔE vs $M(B)$ plane.

After the $B \to \psi(2S)K^*$ event selection, 10–20% of the events have more than one B candidate in the signal area. In these cases, we select the B candidate with minimum $\Sigma(x_i - \mu_i)^2/\sigma_i^2$, where μ_i is a central value of the measured parameter x_i and σ_i is its uncertainty ($B \to l^+l^-K^*$ and $B \to l^+l^-\pi^+\pi^-K^*$ were considered different modes). The following parameters were used where available: the masses of the $\psi(2S)$, K^*, K_S^0, and π^0 candidates, and the identification significance of the kaon candidates from K^* decays and the pion candidates from the $\psi(2S) \to J/\psi\pi^+\pi^-$ decay. The distributions of ΔE vs $M(B)$ for the six different $B \to \psi(2S)K^{(*)}$ decays after all selection criteria are applied are shown in Fig. 1.

The principal sources of background are the cross-feed from a different $B \to \psi(2S)K^{(*)}$ mode or $B \to \psi(2S)K\pi\pi$ modes, the combinatorial background from $\Upsilon(4S) \to B\overline{B}$ decays that do not contain a $\psi(2S)$ daughter, and continuum non-$B\overline{B}$ decays.

Contributions from miscellaneous B decays with $\psi(2S)$ decay products are estimated using the Monte Carlo simulation of $B\overline{B}$ events in which one of the B mesons decays exclusively in the selected mode. The following modes are considered for calculations of background from misidentified B decays to states with charmonium: $B \to \psi(2S)K$ processes with branching fractions obtained in this Rapid Communication (before correcting for this background); $B \to \psi(2S)K^*$ processes with similarly obtained branching fractions and non-resonant contributions to the K^* reconstruction not considered; and $B \to \psi(2S)K\pi\pi$ decays with the value of the

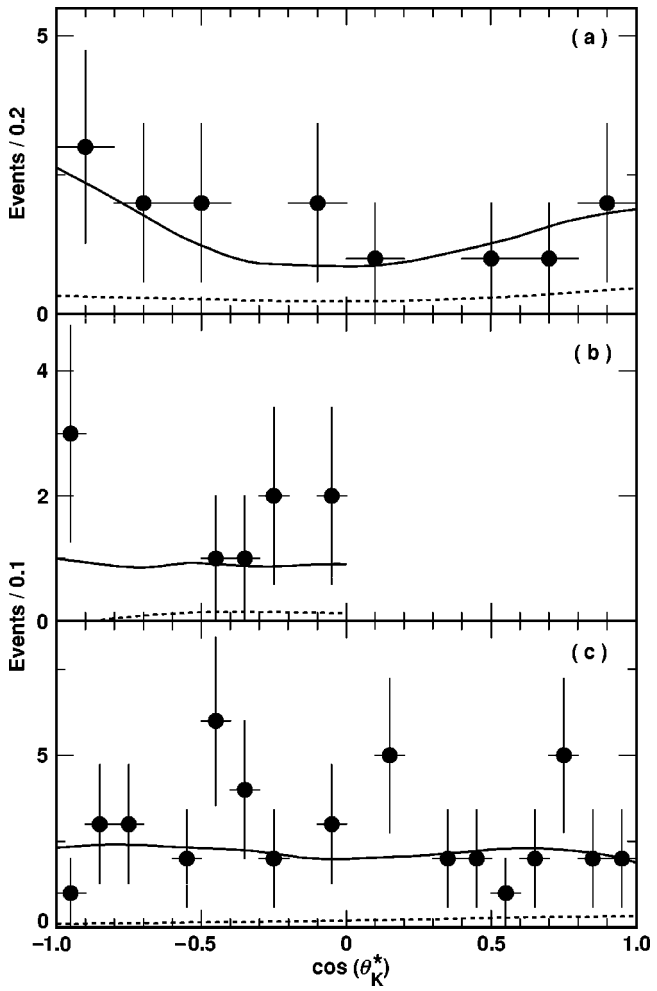

FIG. 2. Spectra of the K^* helicity angles in (a) $B^+\to\psi(2S)K^{*+}$, $K^{*+}\to K^0_S\pi^+$; (b) $B^+\to\psi(2S)K^{*+}$, $K^{*+}\to K^+\pi^0$; and (c) $B^0\to\psi(2S)K^{*0}$, $K^{*0}\to K^+\pi^-$ candidate events in data. The solid curves represent the fit results to the data (points). The dashed curves represent the background contributions.

branching fraction consisting of that for inclusive $B\to\psi(2S)X$ production [18], after the subtraction of K and K^* decay contributions.

The combinatorial background is estimated with fits of the beam-constrained B mass distributions in data. The background shape is obtained with events in the ΔE sideband areas: $0.05<|\Delta E|<0.15$ GeV. As a check, the combinatorial background is also estimated using the $\Upsilon(4S)\to B\bar{B}$ Monte Carlo sample with $B\to\psi(2S)X$ decays excluded. The results of the two methods agree within statistical uncertainty. The results on signal and background yields are summarized in Table I. Lepton universality is assumed in calculations of the efficiencies for the $\psi(2S)\to l^+l^-$ mode.

The decays $B\to\psi(2S)K^*$ are a transition from a pseudoscalar to a pair of vector mesons. The fraction of longitudinal polarization is extracted from the distribution of the K^* helicity angle. The distribution of the K^* helicity angle is given by [19] $d\Gamma/(d\cos\theta_{K^*})\propto\sin^2\theta_{K^*}(1-\Gamma_L/\Gamma)+2\cos^2\theta_{K^*}\Gamma_L/\Gamma$.

Figure 2 shows the K^* helicity angles for the $B^+\to\psi(2S)K^{*+}$, $K^{*+}\to K^0_S\pi^+$; $B^+\to\psi(2S)K^{*+}$, $K^{*+}\to K^+\pi^0$; and $B^0\to\psi(2S)K^{*0}$, $K^{*0}\to K^+\pi^-$ candidate events in data. The $B^0\to\psi(2S)K^{*0}$, $K^{*0}\to K^0_S\pi^0$ data are not used in the polarization measurements because the lack of statistics precludes a reasonable understanding of the background. The curves show the results of the binned likelihood fit to the data. The fit function includes the variable Γ_L/Γ and a fixed amount of background, as listed in Table I. The signal shapes in the fit function for decays with the extreme values of $\Gamma_L/\Gamma=0$ and 1 are extracted from a Monte Carlo simulation. The detector resolution in $\cos\theta_{K^*}$ is ~ 0.06, which is significantly smaller than the bin width. The background shape is estimated using the events from sidebands in the $M(B)$ vs ΔE plane. The results for the fraction of longitudinal polarization, with statistical uncertainties only, are 0.64 ± 0.22, 0.38 ± 0.23, and 0.40 ± 0.14 for the decays with $K^{*+}\to K^0_S\pi^+$, $K^{*+}\to K^+\pi^0$, and $K^{*0}\to K^+\pi^-$ final states, respectively. The correctness of the fit is checked by fitting Monte Carlo generated distributions with a known value of the longitudinal polarization fraction. The probabilities to get greater likelihood values than the observed value are 88, 12, and 10% for these B modes, respectively.

The acceptance and efficiency are evaluated with a simulated sample of $B\to\psi(2S)K^{(*)}$ decays. The contributions to the systematic error come from the uncertainty in the reconstruction efficiency due to track finding (1% per track), lepton and kaon identification (3% per candidate), K^0_S finding (2% per candidate), π^0 reconstruction (3% per candidate), background evaluation (Table I), as well as from uncertainties in the $\psi(2S)$ and J/ψ branching fractions [18]. The Monte Carlo statistical uncertainty is at least a factor of 10 smaller than the statistical uncertainty of the data. Equal pro-

TABLE II. Measured branching fractions $[10^{-4}]$, where the first uncertainties are statistical and the second are systematic. The statistical and uncorrelated systematic uncertainties are added in quadrature in calculations of the average values.

$B^+\to\psi(2S)K^+$	$7.8\pm0.7\pm0.9$
$B^+\to\psi(2S)K^{*+}$, $K^{*+}\to K^0_S\pi^+$	$8.9\pm2.4\pm1.2$
$B^+\to\psi(2S)K^{*+}$, $K^{*+}\to K^+\pi^0$	$9.8\pm3.3\pm1.5$
$B^+\to\psi(2S)K^{*+}$, average	$9.2\pm1.9\pm1.2$
$B^0\to\psi(2S)K^0$	$5.0\pm1.1\pm0.6$
$B^0\to\psi(2S)K^{*0}$, $K^{*0}\to K^+\pi^-$	$7.5\pm1.1\pm1.0$
$B^0\to\psi(2S)K^{*0}$, $K^{*0}\to K^0_S\pi^0$	$12.4\pm7.2\pm1.8$
$B^0\to\psi(2S)K^{*0}$, average	$7.6\pm1.1\pm1.0$

TABLE III. Measured longitudinal polarization fractions, Γ_L/Γ, where the first uncertainties are statistical and the second are systematic. The statistical and uncorrelated systematic uncertainties are added in quadrature in calculations of the average values.

$B^+\to\psi(2S)K^{*+}$, $K^{*+}\to K^0_S\pi^+$	$0.64\pm0.22\pm0.08$
$B^+\to\psi(2S)K^{*+}$, $K^{*+}\to K^+\pi^0$	$0.38\pm0.23\pm0.07$
$B^+\to\psi(2S)K^{*+}$, average	$0.51\pm0.16\pm0.05$
$B^0\to\psi(2S)K^{*0}$	$0.40\pm0.14\pm0.07$
$B\to\psi(2S)K^*$, average	$0.45\pm0.11\pm0.04$

TABLE IV. Comparison of model predictions and experimental results for $R_{\psi(2S)}$ and Γ_L/Γ, where the first uncertainties are statistical and the second are systematic.

Source	$R_{\psi(2S)}$	Γ_L/Γ
Neubert *et al.* [7]	1.85	–
Deshpande and Trampetic [8]	3.8	–
Deandrea *et al.* [8]	2.0	–
Cheng [8]	1.57	0.33
Neubert and Stech [10]	4.35	–
CDF measurement [4]	$1.62\pm0.41\pm0.19$	–
This measurement	$1.29\pm0.22\pm0.05$	$0.45\pm0.11\pm0.04$

duction of charged and neutral B-meson pairs in $\Upsilon(4S)$ decays is assumed. In the cases of decays $\psi(2S)\rightarrow J/\psi\pi^+\pi^-$, the additional systematic uncertainty of 2% comes from the uncertainties involved in the generation of the $\pi^+\pi^-$ invariant mass spectrum. For the modes with K^* daughters, the efficiency depends on the helicity composition of the final state due to the fact that the momenta of the K^* decay products are correlated with the helicity angle. The uncertainty in K^* helicity adds a small contribution of 1% to the systematic uncertainty (the Γ_L/Γ result obtained in this Rapid Communication is used for this estimate). The major sources of systematic uncertainty in the longitudinal polarization fraction measurement are the uncertainties in the fitting procedure (10, 10, 15 %), background estimates (5, 15, 5 %), and differences in detection efficiencies for decays with $\Gamma_L/\Gamma=0$ and 1 (5, 5, 5 %) for modes with $K^{*+}\rightarrow K^0_S\pi^+$, $K^{*+}\rightarrow K^+\pi^0$, and $K^{*0}\rightarrow K^+\pi^-$ final states, respectively.

The results of the measurements are summarized in Tables II and III. The branching-fraction results are $\mathcal{B}(B^+\rightarrow\psi(2S)K^+)=(7.8\pm0.7\pm0.9)\times10^{-4}$, $\mathcal{B}(B^+\rightarrow\psi(2S)K^{*+})=(9.2\pm1.9\pm1.2)\times10^{-4}$, $\mathcal{B}(B^0\rightarrow\psi(2S)K^0)=(5.0\pm1.1\pm0.6)\times10^{-4}$, and $\mathcal{B}(B^0\rightarrow\psi(2S)K^{*0})=(7.6\pm1.1\pm1.0)\times10^{-4}$. These values supersede the previous CLEO results [3] and are in agreement with the CDF measurements [4]. Assuming isospin invariance, we make the first measurement of the longitudinal polarization fraction Γ_L/Γ in the decays $B\rightarrow\psi(2S)K^*$, $\Gamma_L/\Gamma=0.45\pm0.11\pm0.04$, and measure the ratio of vector to pseudoscalar meson production to be $R_{\psi(2S)}\equiv\mathcal{B}(B\rightarrow\psi(2S)K^*)/\mathcal{B}(B\rightarrow\psi(2S)K)=1.29\pm0.22\pm0.05$. Table IV compares experimental results for R and Γ_L/Γ with theoretical predictions [7,8,10]. The predictions for $R_{\psi(2S)}$ of Deshpande and Trampetic [8] and Neubert and Stech [10] are inconsistent with our measurement.

In summary, we have studied all four decays $B\rightarrow\psi(2S)K^{(*)}$ with the $B^0\rightarrow\psi(2S)K^0$ and $B^+\rightarrow\psi(2S)K^{*+}$ modes observed for the first time. The first measurement of the longitudinal polarization fraction is extracted from an angular analysis of the $B\rightarrow\psi(2S)K^*$ candidates. The $B^0\rightarrow\psi(2S)K^{(*)0}$ decays are expected to play a significant role in future CP violation measurements.

We gratefully acknowledge the effort of the CESR staff in providing us with excellent luminosity and running conditions. I.P.J. Shipsey thanks the NYI program of the NSF, M. Selen thanks the PFF program of the NSF, A.H. Mahmood thanks the Texas Advanced Research Program, M. Selen and H. Yamamoto thank the OJI program of DOE, M. Selen and V. Sharma thank the A.P. Sloan Foundation, M. Selen and V. Sharma thank the Research Corporation, F. Blanc thanks the Swiss National Science Foundation, and H. Schwarthoff and E. von Toerne thank the Alexander von Humboldt Stiftung for support. This work was supported by the National Science Foundation, the U.S. Department of Energy, and the Natural Sciences and Engineering Research Council of Canada.

[1] Charge conjugation is implied throughout this Rapid Communication.

[2] ARGUS Collaboration, H. Albrecht *et al.*, Z. Phys. C **48**, 543 (1990).

[3] CLEO Collaboration, M.S. Alam *et al.*, Phys. Rev. D **50**, 43 (1994).

[4] CDF Collaboration, F. Abe *et al.*, Phys. Rev. D **58**, 072001 (1998).

[5] Throughout this Rapid Communication the K^* symbol refers to the $K^*(892)$ meson and the $B\rightarrow\psi(2S)K^{(*)}$ notation represents the following four decays: $B^+\rightarrow\psi(2S)K^+$, $B^+\rightarrow\psi(2S)K^*(892)^+$, $B^0\rightarrow\psi(2S)K^0$, and $B^0\rightarrow\psi(2S)K^*(892)^0$.

[6] M. Wirbel, B. Stech, and M. Bauer, Z. Phys. C **29**, 637 (1985); M. Bauer, B. Stech, and M. Wirbel, *ibid.* **34**, 103 (1987).

[7] M. Neubert *et al.*, in *Heavy Flavours*, edited by A.J. Buras and H. Lindner (World Scientific, Singapore, 1992), p. 286.

[8] N.G. Deshpande and J. Trampetic, Phys. Rev. D **41**, 986 (1990); A. Deandrea *et al.*, Phys. Lett. B **318**, 549 (1993); H.-Y. Cheng, *ibid.* **395**, 345 (1997).

[9] R. Aleksan *et al.*, Phys. Rev. D **51**, 6235 (1995).

[10] M. Neubert and B. Stech, in *Heavy Flavours*, 2nd ed., edited by A.J. Buras and H. Lindner (World Scientific, Singapore, 1998), p. 294.

[11] H.-Y. Cheng and K.-C. Yang, Phys. Rev. D **59**, 092004 (1999).

[12] See, for example, Refs. [10] and [11].
[13] CLEO Collaboration, Y. Kubota *et al.*, Nucl. Instrum. Methods Phys. Res. A **320**, 66 (1992).
[14] T.S. Hill, Nucl. Instrum. Methods Phys. Res. A **418**, 32 (1998).
[15] R. Brun *et al.*, GEANT3 Users Guide, CERN-DD/EE/84-1.
[16] CLEO Collaboration, J.P. Alexander *et al.*, hep-ex/0006002.
[17] Mark III Collaboration, D. Coffman *et al.*, Phys. Rev. Lett. **68**, 282 (1992).
[18] Particle Data Group, D.E. Groom *et al.*, Eur. Phys. J. C **15**, 1 (2000).
[19] M. Jacob and G.C. Wick, Ann. Phys. (N.Y.) **7**, 404 (1959).